AIAA JOURNAL
Vol. 47, No. 10, October 2009

Helmholtz Resonance of Pitot Pressure Measurements in Impulsive Hypersonic Test Facilities

Matthew McGilvray,* Peter A. Jacobs,† Richard G. Morgan,‡ Rowan J. Gollan,§ and Carolyn M. Jacobs§
University of Queensland, St. Lucia, Queensland 4072, Australia

DOI: 10.2514/1.42543

Experimental pitot pressure measurements in impulse facilities have typically had large-scale harmonic fluctuations associated with them. A combined experimental and numerical approach is used to investigate if a Helmholtz resonance is created from the shrouding that protects the pressure sensor from particle impact, rather than from disturbances being present in the freestream. To verify this experimentally, hydraulic oil was used to change the sound speed in the cavity. Numerical calculations of the pitot probe were used to show that both the steady and the expected transient inflow cause a Helmholtz resonance of similar period. However, a 5% isothermal level of freestream noise was required to match the experimental fluctuation levels. Viscous effects were also shown to be significant during the initial transient response of the pressure measurement. A new pitot probe design was successfully tested and shown to be able to reduce the magnitude and period of the fluctuations.

Nomenclature

A_N	=	cross-sectional area of the neck, m^2
a_0	=	sound speed in the cavity, m/s
D	=	diameter of the cavity, m
f_1	=	natural frequency, Hz
L	=	length of the cavity, m
L^*	=	equivalent length of the cavity, m
L_N	=	length of the neck, m
p	=	pressure, Pa
R	=	gas constant, J/kg · K
R	=	radius, m
T_0	=	temperature in the cavity, K
V_0	=	volume in the cavity, m^3
x	=	axial distance, m
γ	=	specific heat ratio
δ	=	shock standoff distance, m
λ	=	wavelength, m
∞	=	freestream

I. Introduction

DUE to tradeoffs in test time and flow replication, a single hypersonic test facility has a limited capability to conduct a full range of aerothermal, materials, and aerodynamic testing [1]. Thus, various types of wind tunnels from long-duration blowdown to impulse-type facilities are used. To match higher-total-enthalpy and higher-total-pressure flows, impulse facilities such as reflected-shock tunnels and expansion tubes become the only choice [2]. Because of the short test times and harsh environment of the flow, measurement of flow properties in impulse facilities, especially of the core flow, becomes increasingly difficult. However, it is still important to accurately measure the flow properties to provide a high level of confidence in the test data from these facilities [3].

Pitot pressure measurements are essential for test flow definition and are a useful diagnostic for confirming if a usable flow exists. Measurements of pitot pressure in impulse facilities have typically exhibited significant fluctuations. However, the average value of a measurement may remain relatively stable over the duration of the test flow. Time-averaging the data has been an acceptable solution for the reflected-shock-tunnel facilities, in which test times are long enough that more than 50 oscillations occur over the test period. In expansion-tube facilities, many conditions appear to have no useful region of steady flow, due to wild oscillations in the pitot pressure signals [4]. However, not all of these oscillations seen in the measurements reflect genuine flow disturbances.

Investigation of this phenomenon in the current study has ruled out both electrical and vibrational effects, concluding that the source of the pressure fluctuations is either in the flow itself or is a result of the way in which the pitot pressure is measured. To ensure survival of the pressure transducers in the pitot probes, shielding is placed in front of the transducer to remove the possibility of particle strikes (usually generated from the diaphragms). Figure 1 shows the pitot probe design used in the University of Queensland expansion-tube facilities, consisting of a cap with a single 2.3 mm hole, a shield with six 1 mm holes on a 3 mm pitch circle diameter, and a sleeve that separates the shield from the transducer face. This arrangement, unfortunately, creates a forward-facing cavity in front of the transducer, in which an acoustic resonance effect can occur.

The cavity in front of the pressure transducer expands out from a neck to a larger volume, similar to a Helmholtz resonator. The natural frequency oscillation of a simple-geometry Helmholtz resonator in subsonic flow [Eq. (1)] is a function of the sound speed, volume, and the neck properties of cross-sectional area and length. Experiments performed on Helmholtz resonance at low supersonic speeds [5,6] ($M < 2$) have shown strong and self-sustaining oscillations characterized by large pressure amplitudes in the cavity and movement of the bow shock. The pressure fluctuates at the base of the cavity due to the added dynamic pressure from movement of the gas back and forth in the cavity through each oscillation period. Therefore, pressures can be obtained above the stagnation pressure of the freestream for part of the oscillation cycle [6]:

$$f_1 = \frac{a_0}{2\pi}\sqrt{\frac{A_N}{V_0 L_N}} \tag{1}$$

Presented as Paper 1157 at the 47th AIAA Aerospace Sciences Meeting, Orlando, FL, 4–8 January 2009; received 3 December 2008; revision received 17 February 2009; accepted for publication 18 February 2009.

*Research Fellow, Centre for Hypersonics, Division of Mechanical Engineering. Member AIAA.
†Senior Lecturer, Centre for Hypersonics, Division of Mechanical Engineering.
‡Professor, Centre for Hypersonics, Division of Mechanical Engineering. Associate Fellow AIAA.
§Ph.D. Candidate, Centre for Hypersonics, Division of Mechanical Engineering. Member AIAA.

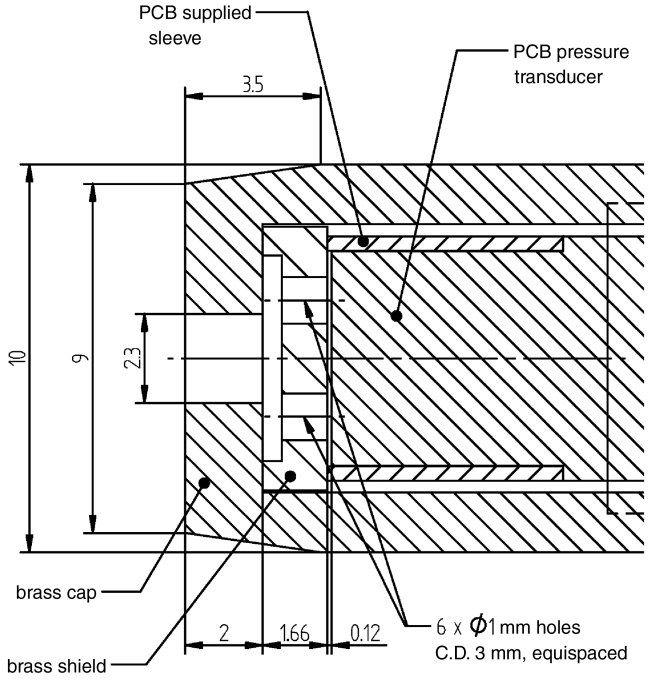

Fig. 1 Expansion-tube pitot pressure transducer mounting arrangement (C.D. denotes the center diameter).

Extensive research at hypersonic freestream speeds of forward-facing cavities on the centerline of blunt bodies has been undertaken by numerous groups looking at reducing nose heating rates and drag in supersonic missiles [7–12]. These studies have focused on Hartmann resonators: a simple cylindrical forward-facing cavity (Fig. 2) exhibiting a periodic fluctuation in pressure at the primary mode frequency given by Eq. (2). This frequency relation includes the effects of shock standoff distance ($L^* = L + \delta$) when compared with the subsonic equivalent [Eq. (1)]:

$$f_1 = \frac{a_0}{\lambda} = \frac{\sqrt{\gamma R T_0}}{4L^*} \tag{2}$$

As most studies have relied upon data taken in facilities in which significant amounts of freestream noise is present (as would be expected in impulsive facilities), Engblom et al. [8] investigated the relationship between the noise and resonance behavior both numerically and experimentally using a quiet facility. For small cavities ($L/D < 1$), it was concluded that the resonance was caused by the freestream noise. However, for deep cavities (large L/D ratios), the flow inside the cavity became self-excited, requiring no freestream noise to produce the fluctuations. The amplitude of the fluctuations was also very consistent, whether or not freestream noise was included in the simulations. As the pitot probe configuration under investigation in this paper has $L/D > 1$, this self-excitation effect is significant. The sensitivity of the amplification of freestream noise to various flow and geometry properties was also studied numerically by Engblom et al. [8]. For a shallow cavity ($L/D = 0.75$), the magnitude of amplification of the noise in the freestream appeared to not be affected greatly by the level of the noise. The maximum amplification of the freestream noise was recorded at a frequency just below the primary frequency of the cavity. Increasing both L/D ratios and freestream Mach number gave larger noise-amplification magnitudes, which was also seen experimentally.

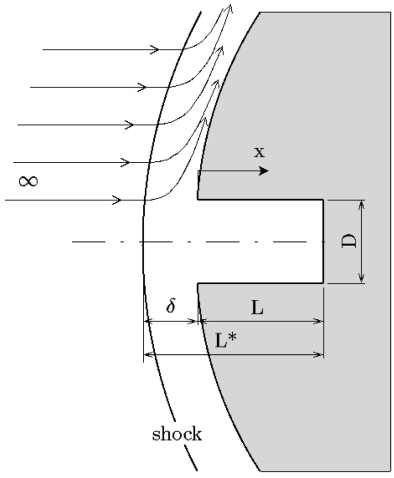

Fig. 2 Schematic of Hartmann resonator in a hypersonic flow.

Most studies have used long-duration testing in which the fluctuations have reached a steady oscillatory pattern and are caused by the freestream noise. With the pitot probe configuration used in impulse facilities, a large initial perturbation arises due to the starting shock wave of the flow. Therefore, the initial startup response of acoustic resonance in forward-facing cavities is of interest, especially as measurements are required from flow startup. Bohachevsky and Kostoff [11] numerically investigated a cavity in front of a sphere in stagnated gas for a steady inflow. In this configuration, the oscillations of the shock wave were initially quite large from the startup shock reflection process. However, after a number of oscillations, the bow shock damped to a steady periodic oscillation. Ladoon et al. [9] experimentally studied the effect of large freestream disturbances on a cavity in which acoustic resonance was present due to small freestream disturbances by photoionizing the flow upstream of the bow shock. Although large oscillations were initially present, these were damped proportionally to a power of the primary oscillation frequency. For large L/D, this damping-decreased and self-sustaining resonance can persist at a larger amplitude than would naturally occur.

The cause of pressure fluctuations observed in a Mach 10 scramjet replication condition in the University of Queensland's X2 expansion tunnel is explored in this paper. Experimental verification of the existence of a Helmholtz resonance in the measurements is explored by changing the physical medium in front of the transducer and also the cavity and neck geometry. To further verify and explore the effect, numerical calculations are then presented of the pitot probe arrangement, with varying inflow properties. They are 1) steady (nominal test-gas properties) 2) transient (properties calculated at the nozzle exit from previous numerical modeling of the facility), and 3) transient (noise overlaid onto freestream properties). Additional calculations are presented for the pitot probe cavity for a Titan atmosphere nonreflected-shock-tube condition, in which the fluctuations are not seen in the experimental measurement.

II. Experimental Measurements of Pitot Pressure

The pitot probe is designed to have a quick response (approximately 10–20 μs [13]) time and protect the pressure transducer from any particle impact. The outer diameter of the probe is usually kept to a minimum to allow probes to be mounted closely together. The pitot rake used in the expansion-tube facilities consists of nine pitot probes, which are spaced 17.5 mm radially apart from each probe's centerline. The axial position of the rake is such that the probes are at the facility exit plane after recoil of the tunnel. PCB Piezotronics piezoelectric transducers are used in the pitot probes at the University of Queensland (11A26 series); the mounting arrangements used in the expansion tubes are shown in Fig. 1. The data from these transducers are recorded on an in-house-designed and in-house-built data recording system, which is able to sample at up to 0.25 μs.

Recently, the operation of a Mach 10 scramjet condition in the X2 expansion tunnel showed a larger oscillatory problem than had previously been noted. After the initial startup of the facility nozzle (before 200 μs), the test gas exhibited oscillations of approximately 35 μs period and 100 kPa amplitude (Fig. 3). The same behavior was seen in multiple shots and across the entire core flow, indicating repeatability of the effect. These fluctuations were much larger (order

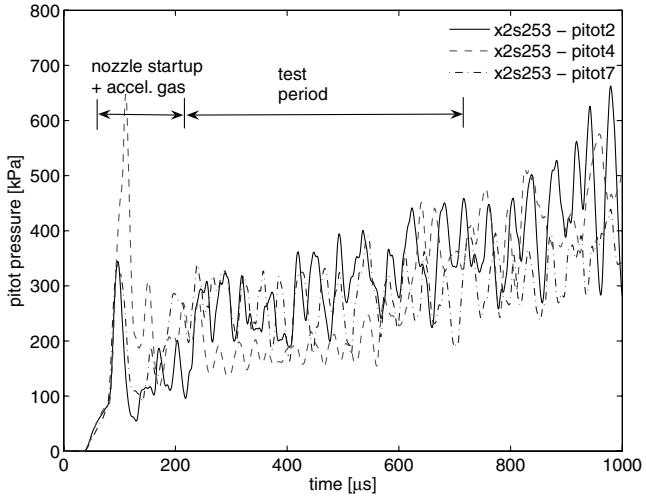

Fig. 3 Experimental pitot pressure measurements at several radial locations for X2 Mach 10 scramjet condition.

of magnitude) than other expansion-tube operating conditions previously established, making us suspect mechanical vibration or electrical noise as possible causes. Response of the PCB Piezotronics transducers is less than 2 μs, and their natural frequency is larger than 400 kHz. Compared with other established expansion-tube flow conditions, the total enthalpy was quite low and the density was high. Therefore, a longer oscillation period can be expected, due to a lower relative sound speed in the probe making the fluctuation more noticeable. Compared with similar reflected-shock-tunnel conditions in the University of Queensland's T4 facility, only 10–15 oscillations occur, due to the short time period, rather than 50–100 oscillations. Thus, a test time is hard to establish, as time-averaging the pitot pressure will give relatively large errors.

These oscillations were of particular concern, as the condition had a ratio of sound speed across the driver/test-gas interface close to where acoustic noise has been found to propagate forward from the free piston driver, corrupting the test flow [4]. However, experiments increasing the sound speed ratio across the interface while keeping similar test flow properties showed similar pitot pressure fluctuations [14]. Computational simulations of the expansion-tunnel flow by McGilvray [14] (Fig. 4) showed lower amplitude and frequency noise over the test period, indicating that the oscillations may not be present in the tunnel exit flow. The simulations also show that the pitot pressure is expected to increase over the test period, as seen in the experiment.

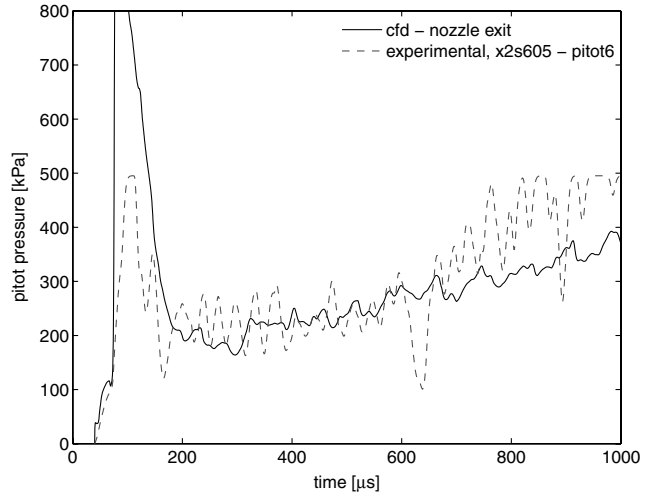

Fig. 4 Comparison of MB_CNS [16] simulation and experimental data for the X2 Mach 10 scramjet condition.

A. Oil-Filled Pitot Probe

To experimentally determine whether a strong Helmholtz resonance effect was present in the pitot probe for the Mach 10 scramjet condition, hydraulic oil was placed into the pitot cavity to alter the oscillatory frequency. This allows both the geometry and the freestream gas properties to remain unchanged; only the sound speed of the fluid in the cavity is modified. However, this will not necessarily give an indication of the noise present in the freestream, as the cavity may still produce some resonance.

The hydraulic oil was placed into the cavity through a hypodermic syringe while mounted in the test section, with the fluid's surface tension holding the oil in the cavity. Although care was taken, it cannot be assured that no air is present in the cavity. Some of this oil could also leak from the cavity as the flow impinges the probe. The results shown in Fig. 5, in which probes are located 17.5 mm radially apart, show t hat the frequency of fluctuations decreased when oil was placed inside the cavity. Performing a power spectrum density analysis, the dominant frequency of the noise can be clearly seen to shift from 30 to approximately 55 kHz (Fig. 5b). The amplitude of the pressure fluctuations slightly decreased. This same behavior was noted across several tests and across various pitot locations. These results indicate that a strong Helmholtz resonance is present in the cavity.

B. Swirl-Cap Pitot Probe

Turbine engine combustion processes are quite often susceptible to similar axial thermoacoustic effects. To overcome this, vorticity is

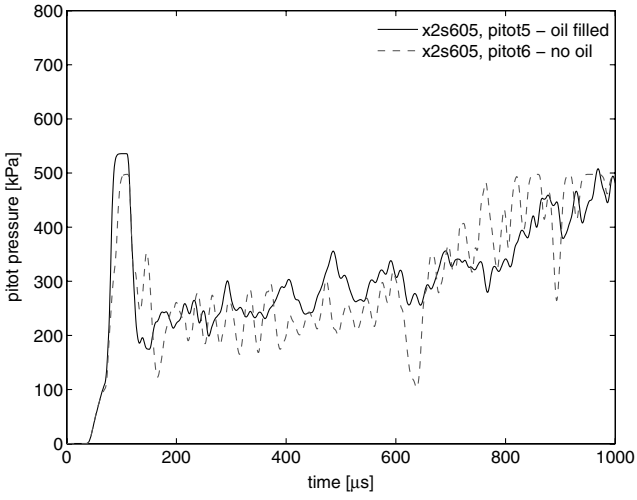

a) Pitot pressure

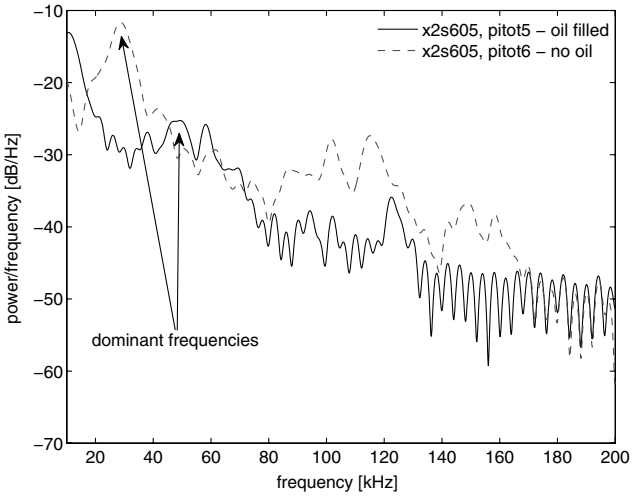

b) Power spectral density analysis

Fig. 5 Effect of filling the pitot probe cavity with hydraulic oil.

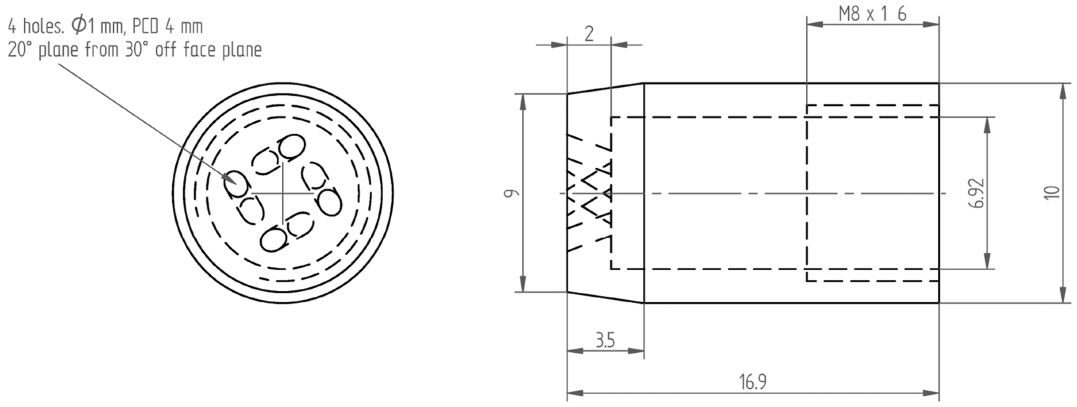

Fig. 6 Schematic of the swirl-cap design used in the experiment (PCD denotes pitch circle diameter).

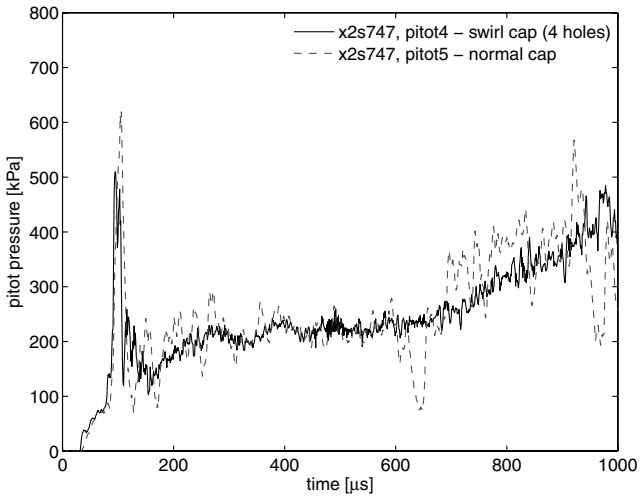

a) Test flow

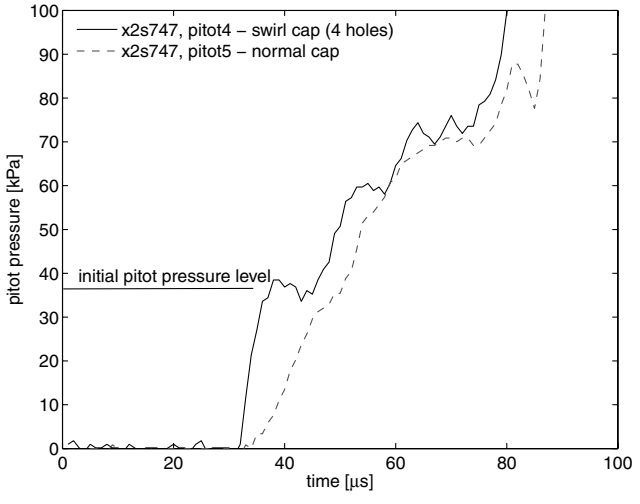

b) Initial rise period

Fig. 7 Effect of using a swirl cap on pitot pressure measurement.

usually introduced into the flow to break up the wave structure as it moves down the length of the combustor [15]. This same principle has been applied for the pitot pressure oscillation problem by manufacturing a pitot probe cap in which the holes allow the flow through to the transducer while inducing swirl into the flow. The design used (Fig. 6) has four 1.2 mm holes through the front cap at a diameter of 5 mm and an angle of 30 deg to the freestream. With the swirl-cap design, the direct impact of particles onto the transducer is not possible. This allows removal of the shield from the probe, thus reducing the volume of the cavity.

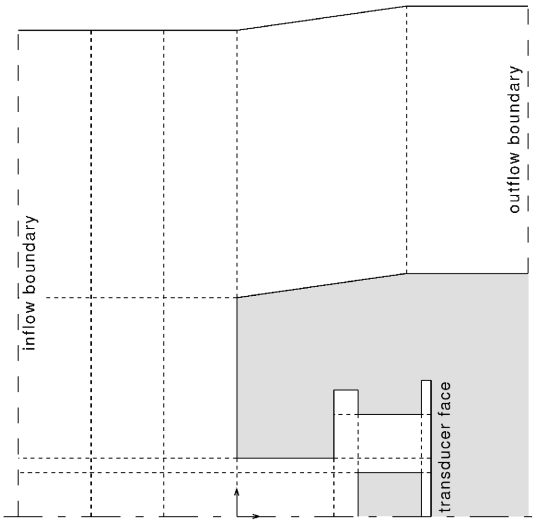

Fig. 8 Schematic of numerical setup for expansion-tube pitot probe cavity calculations.

Using the swirl cap for the Mach 10 scramjet condition in the X2 facility removed the long-time-base periodic fluctuations previously seen in the pitot pressure measurements (Fig. 7). These have been replaced with a higher-frequency (5 μs) and lower-amplitude resonance, which would be expected for the small volume after the intake holes. Although there is still some long-time-base unsteadiness in the flow, with deviations of approximately 10 kPa, this is reduced by an order of magnitude from the original pitot cap measurements. The use of the swirl-cap design has an additional benefit of reducing the initial rise time from 10–20 [13] to 3–5 μs, shown in Fig. 7b. However, there now appears to be some high-frequency noise in the initial gauge response time.

III. Numerical Investigation

To both verify and investigate the source of the fluctuations in experimental pitot pressure, the pitot probe arrangement was simulated numerically using the University of Queensland's two-

Table 1 Inflow, initial fill, and stagnation conditions for the Mach 10 scramjet condition in chemical equilibrium

	Inflow	Initial fill	Stagnation
Pressure, kPa	2.31	0.14	317
Temperature, K	245	300	3512
Axial velocity, m/s	3190	0	0

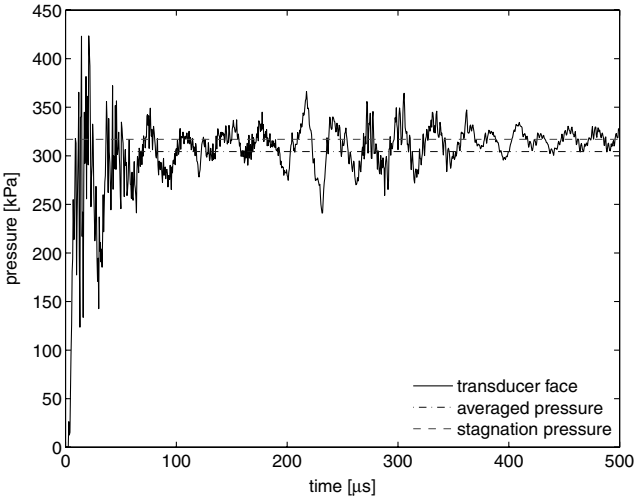

Fig. 9 Static pressure at the pitot probe transducer face for steady inflow at the Mach 10 scramjet condition. Stagnation pressure is that calculated behind the bow shock over an axially aligned cylinder.

dimensional/axisymmetric MB_CNS flow solver [16]. This is an explicit, cell-centered finite volume, Navier–Stokes solver that uses a structured grid. This code was developed for calculating hypersonic flows in which large gradients are present in the flow.

To decrease the computational expense, a simplified axisymmetric geometry was used rather than three-dimensional. Thus, the six holes through the shield were incorporated into the simulation by retaining the hole's inner and outer radii (0.9 and 2.1 mm), creating a singular annular gap in the shield, shown in Fig. 8. This maintains a direct line of sight of the gas onto the transducer face. However, this meant that the cross-sectional area of the holes increased by a factor of 1.66. Simulations in which the area of the holes was conserved at the offcenter radius (inner radius is 1.14 mm and outer radius is 1.18 mm) showed little change in the response of the pressure in the cavity.

The grid resolution required in this simulation is determined by the ability to resolve the surface pressure, shock movement, and acoustic waves. A cell size of 10^{-2} mm both inside and in front of the cavity was used. This is the same cell size as used by Engblom et al. [8] in calculating a simple forward-facing cavity in flows up to Mach 9. With the wavelength of the fluctuations larger than four times the cavity length ($\lambda = 4L^*$), the grid is easily fine enough to meet the criterion of 40 cells per wavelength used by Engblom et al. when only considering the 2 mm length of the neck. This grid resolution should also be sufficient to accurately capture the movement of the bow shock, as the movement is found to be between 0.2 and 0.8 mm during one oscillation cycle (20–80 cells). Lower grid resolution simulations showed similar flow effects to those presented here, although the fluctuations were damped more rapidly.

It was concluded by Engblom et al. [8] that the viscous effects are minimal for simple forward-facing cavities. This led to inviscid calculations being conducted to decrease the computational expense of the calculations. However, as will be shown in the calculation of the Titan nonreflected-shock-tube condition, the viscous effects are important in the initial period, in which the mass of gas in the cavity is rapidly increasing and the gas is quite hot.

Any chemistry effects in the flow are assumed to be in a state of equilibrium for the following reasons:

1) The inflow for the simulation, taken as the expansion-tunnel exit flow for a Mach 10 scramjet condition, is expected to be in equilibrium.¶

2) There is a large flow residence time for the gas after being shock-processed by the pitot probe bow shock, until being brought to rest in the cavity.

The equilibrium chemistry was included into the MB_CNS simulation by linear interpolation of a lookup table created from the chemical equilibrium analysis (CEA) code [17] for various temperatures and densities.

All the pressure plots presented at the transducer face have been determined by integration of the pressure with surface area [Eq. (3)]. This is to account for the fact that the transducer effectively measures the average pressure on the diaphragm:

$$p_{\text{transducer}} = \frac{\int_0^R p \, \mathrm{d}A}{\pi R^2} \tag{3}$$

IV. Steady Inflow Simulation

The simulation was undertaken using a steady inflow boundary condition (which is effectively the freestream state) along the left-hand boundary, as shown in Fig. 8. Thus, no freestream noise is present and the only excitation of fluctuations within the cavity should be due to the initial shock. The inflow conditions for the calculation are taken as the average flow conditions from a simulation of the Mach 10 condition in the X2 facility by McGilvray [14]. These are shown in Table 1, along with the initial fill and expected stagnation conditions. These stagnation conditions (behind the bow shock) were established from a simulation in which the cavity was removed (i.e., blunt-body cylinder).

The large pressure fluctuations noted experimentally appear in the pressure calculated at the transducer face (Fig. 9). This behavior can be seen throughout the entire simulation time, which is equivalent to the experimental test period (500 μs). Using the time between 60 and 350 μs, the period of the fluctuations is calculated to be 31.25 μs (eight fluctuations). The amplitude of these oscillations varies throughout the simulation, with a maximum of 120 kPa (ignoring the first oscillation). The magnitude is seen to dampen by the end of the simulation. Both a high- and a low-frequency oscillation can be seen in the pressure trace. The averaged pressure after 60 μs is 304.5 kPa, which is 4% lower than the actual pitot pressure of the freestream.** Thus, a significant error in the test flow conditions can be made if an averaged pressure is used. However, this may not be as large with longer-test-period flow, in which more oscillations will occur over the test period.

The flowfield is investigated at different times over one fluctuation period in the simulation, using contours of static pressure (Fig. 10). The shock is seen to curve around the front of the probe, becoming normal at the centerline and having a distinct change in the radius of curvature toward the top of the probe before becoming quite conical above the probe. This change of shock curvature is not observed when the cavity is not included (i.e., blank cylinder). The position of this shock is seen to first move closer toward the probe and then to back away from the probe. A section of the neck region in the pitot probe exhibits a lower pressure (Fig. 10), which moves in sequence with the bow shock. Smaller vortical structures also exist in the pitot cavity that move during the oscillation period.

The centerline shock standoff from the front of the probe throughout the simulation is shown in Fig. 11, in which the maximum oscillation is 0.8 mm. The period of the oscillations is approximately 31 μs, which is close to that seen in the pressure oscillations. As seen in the static pressure at the transducer face (Fig. 9), the fluctuations in the position of the shock are seen to dampen toward the end of the simulation. The four large oscillations during the middle of the simulation also reflect the large pressure fluctuations during the same time period. The phase between the pressure fluctuations and the movement of the bow shock is half a period (16 μs), so that when the pressure at the transducer face is at a maximum, the shock standoff is at a minimum. With these observations, the oscillations in the transducer face pressure are linked to the movement of the bow shock.

To investigate the flowpath of the freestream gas and the stagnated gas, contour plots of axial velocity are shown in Fig. 12, with path lines overlaid. The two times shown correspond to the minimum and maximum pressure at the transducer face. There is a large near-zero velocity (stagnation) region that exists in front of the probe. This

¶Ignoring nonequilibrium effects in the nozzle startup flow.

**Pressure averaging is done over a period after startup.

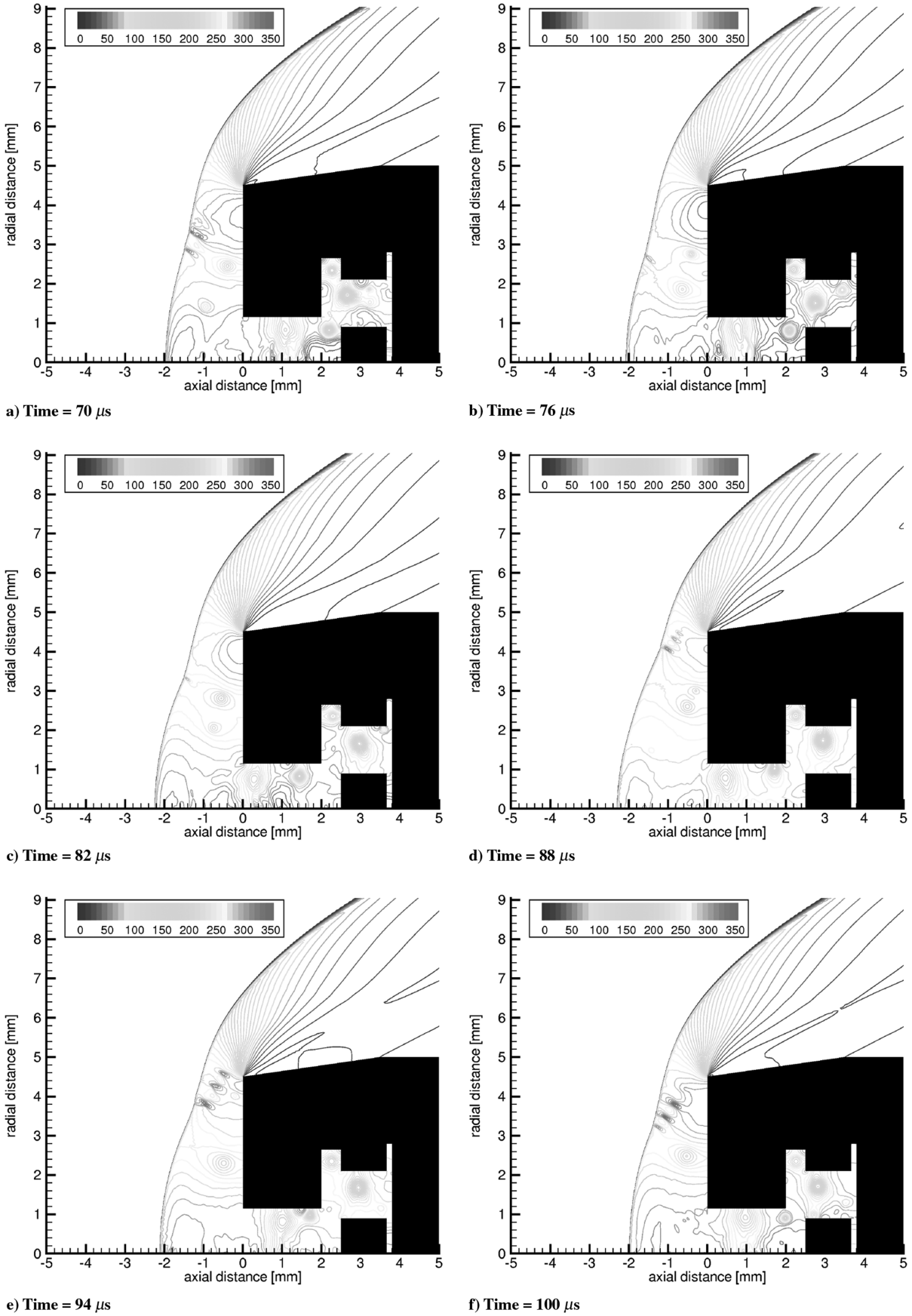

a) Time = 70 μs **b) Time = 76 μs**

c) Time = 82 μs **d) Time = 88 μs**

e) Time = 94 μs **f) Time = 100 μs**

Fig. 10 Static pressure contours of the pitot probe for various times through one oscillatory period. Pressure units are kPa.

region is larger both radially and axially when the shock standoff distance is at a maximum compared with the minimum. The distinct change in the radius of curvature noted previously corresponds to the radial position of the edge of the stagnation region. The drops in static pressure within the cavity can now be seen to be the vorticity in the flow. The grid resolution is such that each vortex is resolved over 30 finite volume cells. Although the simulation was nominally inviscid, the numerical dissipation inherent in the code damps the vortices.

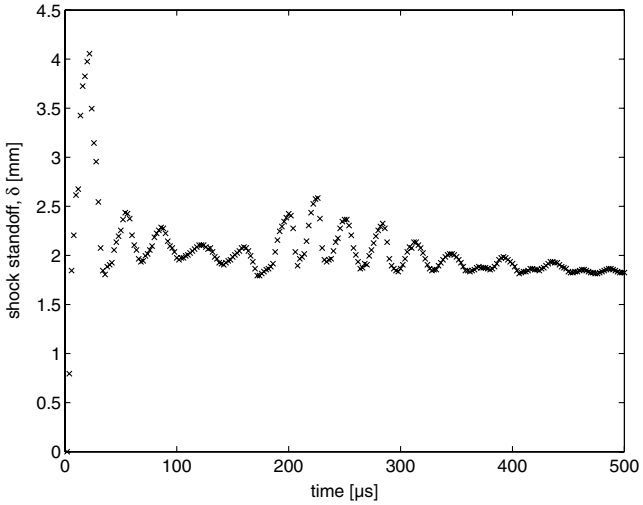

Fig. 11 Shock standoff distance from pitot probe simulation using steady inflow for the Mach 10 scramjet condition.

We have not yet experimented with much higher grid resolutions and viscous simulations to see the point at which physical dissipation of molecular diffusion takes over as the dominant damping mechanism. The importance of physical dissipation is shown later in Sec. VI.

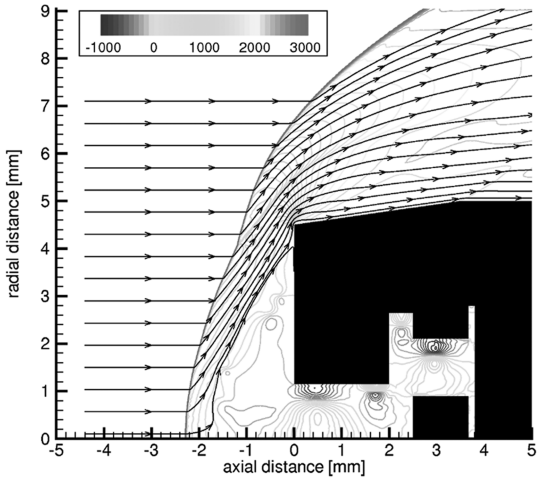

a) Time = 88 μs

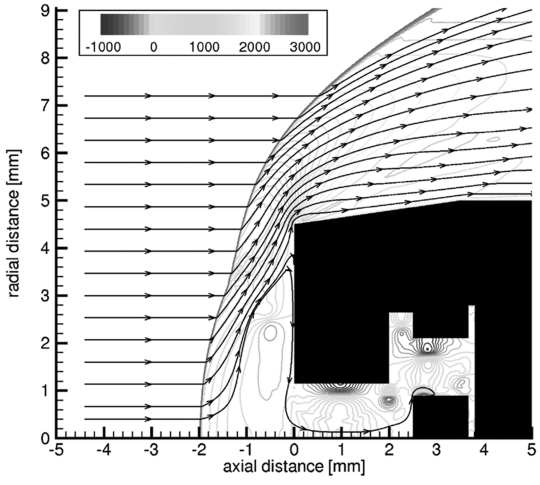

b) Time = 100 μs

Fig. 12 Axial velocity contour of pitot probe with path lines overlaid assuming a steady flowfield. Velocity units are in meters/second.

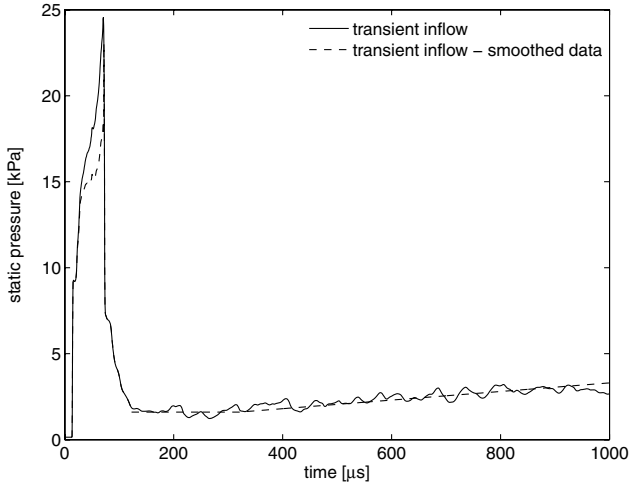

a) Static pressure

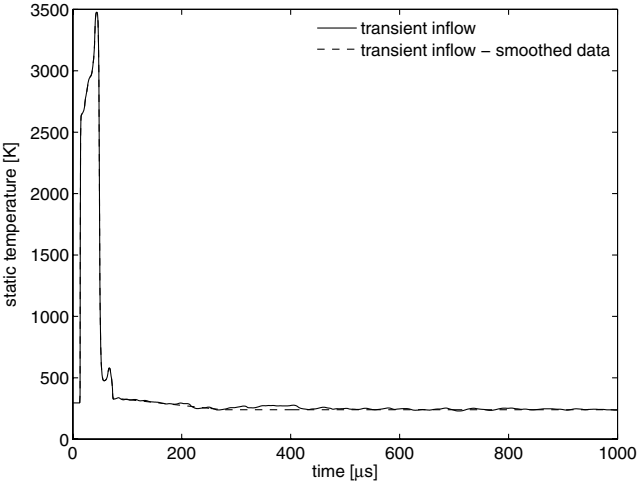

b) Static temperature

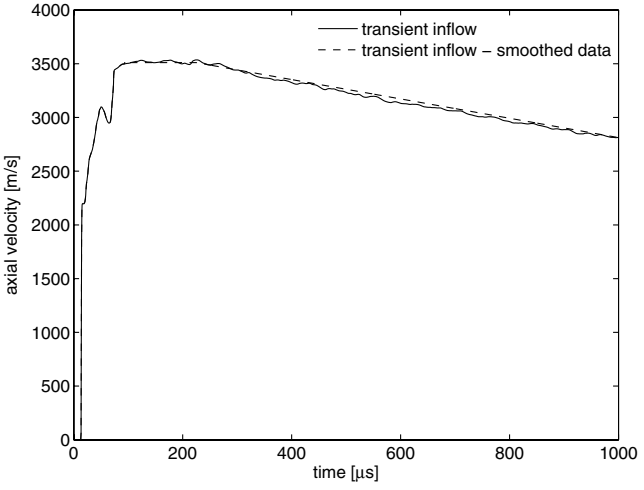

c) Axial velocity

Fig. 13 Inflow properties for the transient simulation. Adapted from calculations presented in [14] of the X2 Mach 10 scramjet condition.

Therefore, as the momentum of the gas grows within the cavity (due to the pressure at the transducer face being larger than that of the freestream), the shock moves away from the pitot body (due to the stagnated region in front of the pitot increasing in geometric size). This causes the pressure at the transducer face to decrease below the freestream pitot pressure. Then, as the momentum of the gas in the cavity decreases below the momentum of the gas that has been

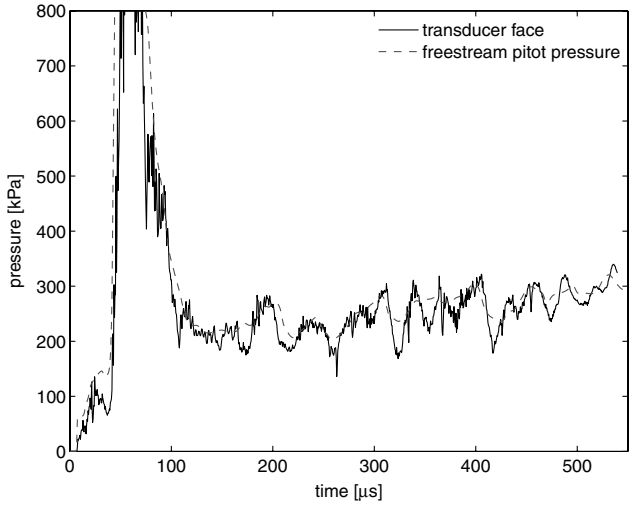

a) Comparison to computational freestream

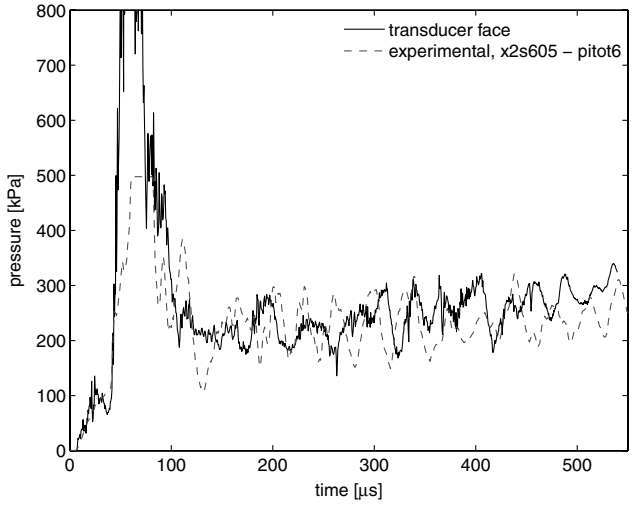

b) Comparison to experimental

Fig. 14 Static pressure at the transducer face from transient inflow simulation of the Mach 10 scramjet condition. This uses the nominal inflow data from Fig. 13.

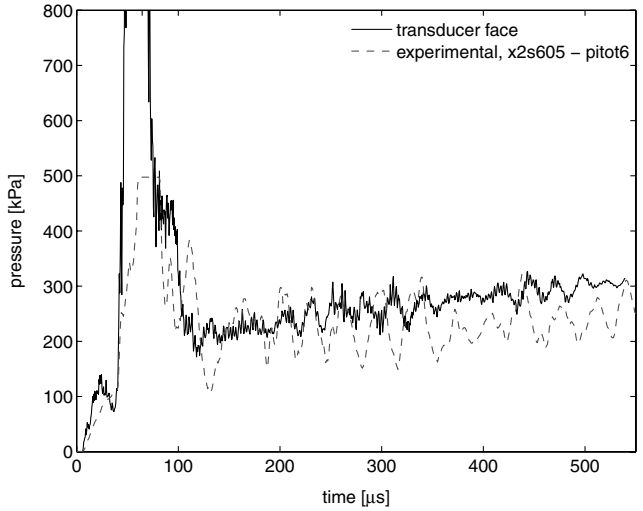

Fig. 15 Static pressure at the transducer face from 0% freestream noise transient inflow simulation of the Mach 10 scramjet condition. This uses the smoothed inflow data from Fig. 13.

shocked, the stagnation region starts to decrease in front of the probe, decreasing the shock standoff distance and accelerating the gas toward the transducer in the cavity. This process is then repeated, damping out with time.

V. Transient Inflow Simulation

As the test flow produced in the expansion-tunnel facility is preceded by both a slug of acceleration gas (high sound speed and same velocity and static pressure as the test gas) and gas processed by nozzle startup waves, the steady inflow simulation does not precisely reproduce the experiment, as the flow starting is modeled as a single discontinuity. To more closely match the experimental flow, a transient inflow boundary condition was implemented using the expansion-tunnel exit flow from an MB_CNS simulation of X2 [14]. The time history of the inflow variables is given in Fig. 13, in which the initial fill properties in the simulation are the same as those of the steady inflow simulation (Table 1). After the passing of the acceleration gas and the nozzle startup gas ($\sim$150 μs), a period of reasonably steady flow ($\sim$150–300 μs) is created before the pressure is seen to rise and the velocity decrease. Slight oscillations are present in all flow properties, which are a feature of the unsteady flow of the physical facility, but may also be a discrepancy in the numerical calculation, due to the large size of the calculation [14,18]. These fluctuations represent an oscillation in pitot pressure of approximately 30 kPa with a period of 60 μs (Fig. 4), although neither the period nor the amplitude are truly repetitive.

A comparison of the static pressure at the transducer face with the pitot pressure of the freestream in Fig. 14a, in which the freestream pitot pressure is calculated at each time interval using CEA,[††] shows large-scale deviations from freestream during the test time. However, these seem to follow the fluctuations of the inflow rather than the 30 kHz, 100 kPa frequency that was seen experimentally (Fig. 14b). The initial startup process is also not captured well in the simulation, with fluctuations occurring during the passage of the acceleration gas. With the significant mass flow into the cavity, there will be large viscous effects associated with the high velocities. After the cavity is filled, little mass enters or exits the cavity and the inviscid effects dominate the flowfield.

With the previous transient numerical simulation not accurately matching the level of fluctuations and dominant frequency in the experimental measurements, further numerical simulations were conducted to investigate the effect that the inflow noise (i.e., freestream) has on the pressure fluctuations at the transducer face. Initially, the inflow was smoothed using linear segments after the startup flow, to determine the scale of the fluctuations with no freestream noise (i.e., 0% noise). The results from this simulation can be seen in Fig. 15, in which the 30 kHz fluctuation is now dominant compared with the initial numerical simulation. Thus, the resonant frequency of the cavity in the steady inflow simulations reflects that measured experimentally. However, the amplitude of the pressure fluctuations is now approximately half of that seen experimentally. In comparison to the steady inflow simulations, this behavior indicates the importance of the flow starting process on the level of fluctuations.

With the smoothed inflow data simulations unable to reach the amplitude of the experimental measurements, this indicates that some level of noise must be present in the freestream. Following the work conducted by Engblom et al. [8], the addition of numerical noise to the base signal (i.e., the smoothed transient inflow data) can increase the amplitude. The Helmholtz resonance response of the cavity acts to amplify the freestream noise, although the amplification factor does not vary greatly with the level of freestream noise. This is different from the initial noise seen in the transient inflow (Fig. 13), as the fluctuations are now added in a consistent manner.

The numerical noise used consists of in-phase sinusoidal variations of pressure and density, while maintaining a constant freestream temperature (isothermal). This represents a one-dimensional axial wave pattern with no radial variations. This noise

[††]Pitot pressure calculation uses a shock problem, then brings the gas to rest isentropically using a series of pressure-entropy problems.

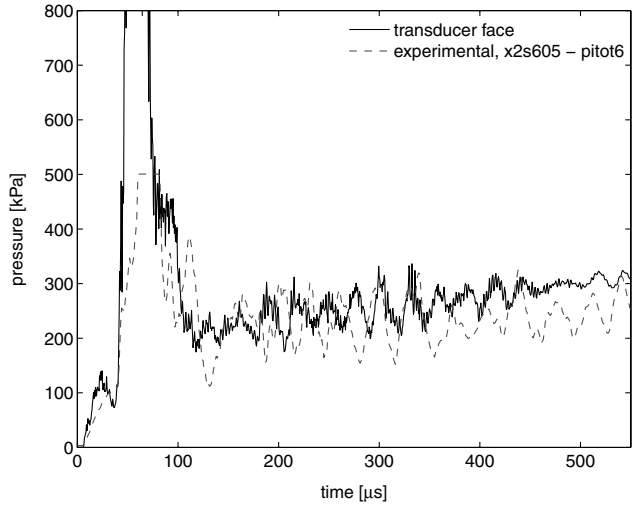

a) 2% freestream noise

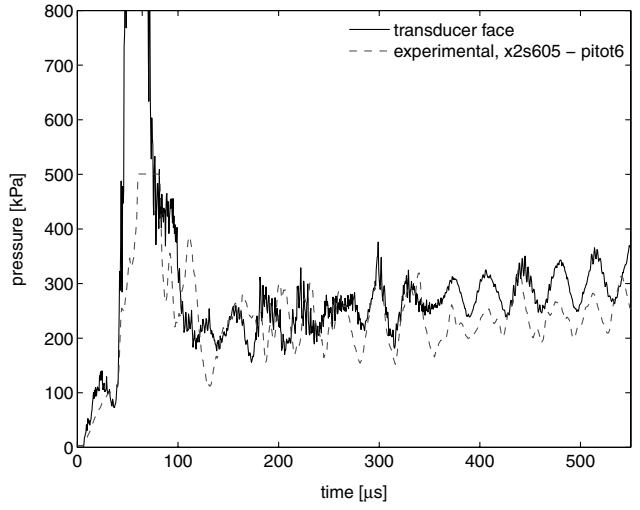

b) 5% freestream noise

Fig. 16 Static pressure at the transducer face from *noise addition* transient inflow simulation of the Mach 10 scramjet condition. This uses the smoothed inflow data from Fig. 13, with differing levels of isothermal noise overlaid.

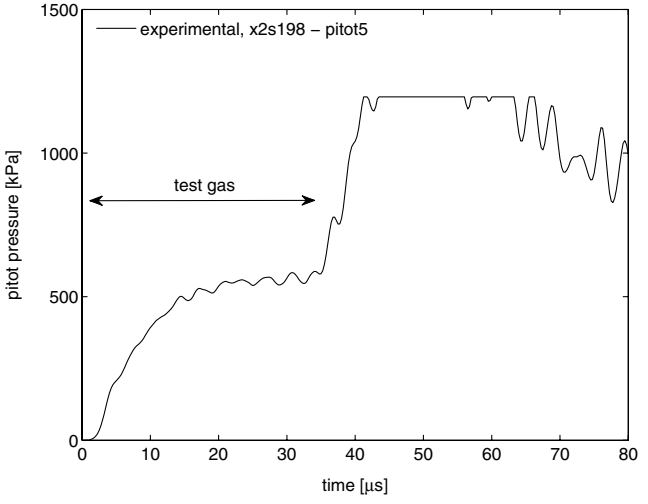

Fig. 17 Experimental pitot pressure measurement for the X2 7 km/s nonreflected-shock-tube Titan condition.

is implemented directly after the startup waves (at 120 μs in Fig. 13). Engblom et al. [8] found that the amplification of the freestream noise was a maximum when the frequency of the numerical noise was 8% less than the primary frequency of the cavity. To predict the lowest level of freestream noise present experimentally, the period of the freestream noise implemented was 36 μs. The rms levels of 2 and 5% were investigated for this noise. The results for the simulation with artificial noise overlaid can be seen in Fig. 16, in which the 5% case shows the closest match to the experimental data. The addition of 5% noise maintains the same period of oscillation as the experiment and the 0% freestream noise transient inflow case, while now matching the amplitude of the fluctuations. Given the assumptions made in the simulation, the experimental freestream noise rms value is likely to be $\sim$5%.

VI. Titan Entry Condition: Nonreflected-Shock-Tube Mode

Recently, the X2 expansion-tube facility has also been used as a nonreflected-shock tube to investigate radiation in the nonequilibrium region behind a normal shock. Thus, the volume of gas immediately behind the shock is that used during the experiment. Similar to the experimental results for the Mach 10 expansion-tunnel condition, the pitot pressure is recorded at the tube exit. This pitot pressure trace also exhibits a slow rise time (Fig. 17); however, no

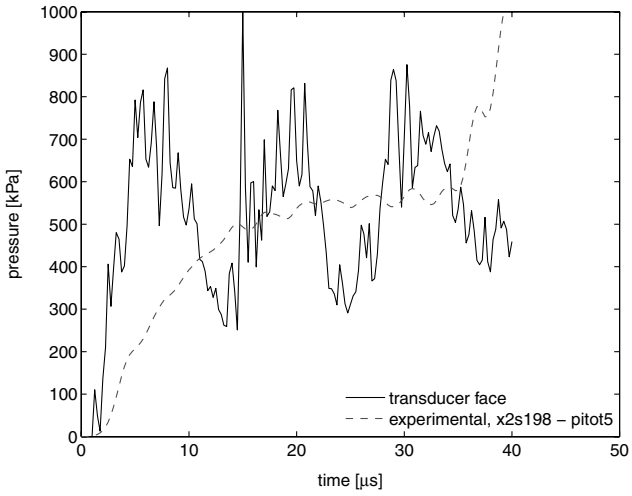

a) Inviscid simulation

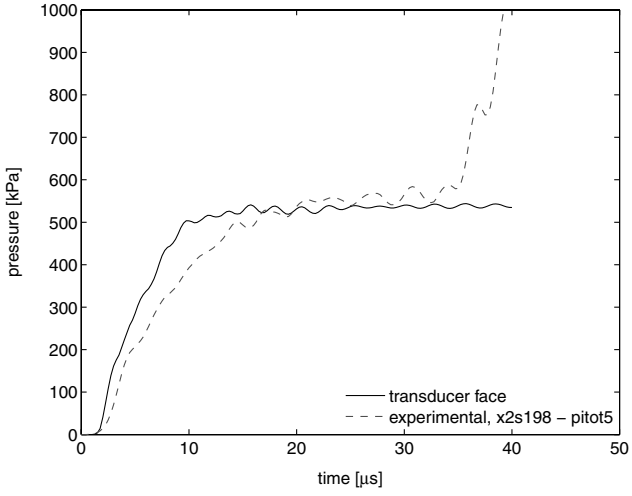

b) Viscous simulation

Fig. 18 Static pressure at transducer face from steady inflow simulation of the X2 7 km/s Titan condition.

oscillations in the pressure signal are present during this period [19]. Looking at previous expansion-tube experimental data (including that presented for the Mach 10 scramjet condition for X2), little freestream fluctuation can be seen in this initial gas slug. However, the numerical calculations for both the steady and the transient inflow Mach 10 condition show fluctuations in this period (Figs. 9 and 15).

To explore this further, a numerical simulation was conducted using the geometry/grid previously described for the pitot probe for an 80 Pa, 7 km/s Titan gas condition (95%N_2/5%CH_4 by volume), with the pitot pressure for this condition shown in Fig. 17. This case differs from that previously calculated, as the freestream is known to be in a state of nonequilibrium. Once stagnated, however, the gas composition will be in a state of chemical equilibrium. Therefore, to reduce the size of the calculation, the gas was again assumed to be in chemical equilibrium. The inflow conditions were calculated using CEA [17], which gave flow properties of 40.7 kPa, 6434 K, and 6578 m/s.

As shown in Fig. 18, the inviscid calculation exhibits the large pressure fluctuations at the transducer face. The response time is also much shorter than the experimental pitot pressure measurement by over 10 μs. With the viscous terms included in the calculation (on the same grid), the fluctuations are removed and the result is a closer representation of the experimental measurements. This indicates the importance of the viscous terms when the pitot cavity is initially filling to dampen out the initial perturbation of the shock. The viscous effects also limit the flow into the cavity, lowering the response time of the measurement.

VII. Conclusions

Large fluctuations in experimental pitot pressure measurements in impulse facilities have been shown to be caused by a Helmholtz resonance effect. This is due to the geometry of the pressure transducer mounting and large perturbations provided by shocks and discontinuities during the startup period of these facilities. Larger amplitudes are recorded for flow conditions that have a relatively high freestream density and Mach number.

Numerical calculations were used to investigate the flow in the pitot cavity for a Mach 10 expansion-tunnel condition. Steady inflow calculations showed a similar amplitude, and frequency pressure oscillation was present at the transducer face. However, when the transient history of the startup process was included in the inflow of the simulation, the amplitude was seen to drop. A 5% rms level of isothermal inflow noise was required to replicate the amplitude of the experimentally observed pressure fluctuations. By simulating a nonreflected-shock-tube condition, the viscous effects in the cavity were found to dominate the initial fill of the cavity, limiting the measurement response and dampening the initial shock perturbation.

To overcome the pressure fluctuations, a new design for the transducer shielding was experimentally tested, in which the volume of the cavity was reduced and the throat section was separated into four holes with an offaxis orientation. This design was able to remove a bulk of the large-scale fluctuations previously recorded and improve response time and is recommended by the authors for high-accuracy measurements.

Acknowledgments

The authors would like to acknowledge the financial support of the Australian Research Council for the experiments. Financial support for the cluster computer was provided by SUN Microsystems and by the Queensland State government under the Smart State program. All the simulations detailed in this paper were undertaken on the Blackhole cluster computer located at the Centre for Hypersonics, University of Queensland. We thank Daniel Potter, Rainer Kirchhartz, and Wilson Chan for running the University of Queensland cluster computer.

References

[1] Bushnell, D., *Advanced Hypersonic Test Facilities*, Progress in Astronautics and Aeronautics, Vol. 198, AIAA, Reston, VA, 2002, Chap. 1.

[2] Chinitz, W., Erdos, J., Rizkalla, O., Anderson, G., and Bushnell, D., "Facility Opportunities and Associated Stream Chemistry Considerations for Hypersonic Air-Breathing Propulsion," *Journal of Propulsion and Power*, Vol. 10, No. 1, 1994, pp. 6–17. doi:10.2514/3.23705

[3] Park, C., "Validation of CFD Codes for Real-Gas Regime," AIAA Paper 97-2530, 1997.

[4] Paull, A., and Stalker, R., "Test Flow Disturbances in an Expansion Tube," *Journal of Fluid Mechanics*, Vol. 245, 1992, pp. 493–521. doi:10.1017/S0022112092000569

[5] Smith, T., and Powell, A., "Experiments Concerning the Hartmann Whistle," Dept. of Engineering, Univ. of California, Los Angeles, TR 64-42, Los Angeles, 1964.

[6] Jungowiski, W., and Grabitz, G., "Self-Sustained Oscillation of a Jet Impinging Upon a Helmholtz Resonator," *Journal of Fluid Mechanics*, Vol. 179, 1987, pp. 77–103. doi:10.1017/S0022112087001447

[7] Engblom, W. A., Yuceil, B., Goldstein, D. B., and Dolling, D., "Experimental and Numerical Study of Hypersonic Forward-Facing Cavity Flow," *Journal of Spacecraft and Rockets*, Vol. 33, No. 3, May–June 1996, pp. 353–359. doi:10.2514/3.26767

[8] Engblom, W. A., Goldstein, D. B., Ladoon, D., and Schneider, S., "Fluid Dynamics of Hypersonic Forward-Facing Cavity Flow," *Journal of Spacecraft and Rockets*, Vol. 34, No. 4, July–Aug. 1997, pp. 437–444. doi:10.2514/2.3255

[9] Ladoon, D. W., Schneider, S. P., and Schmisseur, J. D., "Physics of Resonance in a Supersonic Forward-Facing Cavity," *Journal of Spacecraft and Rockets*, Vol. 35, No. 5, Sept.–Oct. 1998, pp. 626–632. doi:10.2514/2.3395

[10] Huebner, L., and Utejra, L., "Mach 10 Bow-Shock Behaviour of Forward-Facing Nose Cavity," *Journal of Spacecraft and Rockets*, Vol. 30, No. 3, May–June 1993, pp. 291–297. doi:10.2514/3.25513

[11] Bohachevsky, I., and Kostoff, R., "Supersonic Flow over Convex and Concave Shapes with Radiation and Ablation Effects," *AIAA Journal*, Vol. 10, No. 8, Aug. 1972, pp. 1024–1031. doi:10.2514/3.50289

[12] Marquart, E., Grubb, J., and Utreja, L., "Bow Shock Dynamics of a Forward Facing Cavity," AIAA Paper 87-2709, 1987.

[13] Sutcliffe, M., and Morgan, R., "The Measurement of Pitot Pressure in High Enthalpy Expansion Tubes," *Measurement Science and Technology*, Vol. 12, 2001, pp. 327–334. doi:10.1088/0957-0233/12/3/312

[14] McGilvray, M., "Scramjet Testing at High Enthalpies in Expansion Tube Facilities," Ph.D. Thesis, Univ. of Queensland, St. Lucia, QLD, Australia, 2008.

[15] Eldredge, J. D., and Dowling, A. P., "The Absorption of Axial Acoustic Waves by a Perforated Liner with Bias Flow," *Journal of Fluid Mechanics*, Vol. 485, 2003, pp. 307–335. doi:10.1017/S0022112003004518

[16] Jacobs, P., "MB_CNS: A Computer Program for the Simulation of Transient Compressible Flows," Dept. of Mechanical Engineering, Univ. of Queensland, Rept. 10/96, St. Lucia, QLD, Australia, 1996.

[17] McBride, B., and Gordon, S., "Computer Program for Calculation of Complex Chemical Equilibrium Compositions and Applications 2: Users Manual and Program Description," NASA Ref. Publ. 1311, 1996.

[18] Wilson, G., Sussman, M., and Bakos, R., "Numerical Simulations of the Flow in the HyPULSE Expansion Tube," NASA, TM 110357, June 1995.

[19] Gollan, R., Jacobs, C., Jacobs, P., Morgan, R., McIntyre, T., Macrossan, M., Buttsworth, D., Eichmann, T., and Potter, D., "A Simulation Technique for Radiating Shock Tube Flows," *Proceedings of the 26th International Symposium on Shock Waves*, Vol. 1, edited by K, Hannemann and F. Seiler, Springer, Berlin, 2009, pp. 465–470. doi:10.1007/978-3-540-85168-4

N. Chokani
Associate Editor